Coupling of lipolysis and de novo lipogenesis in brown, beige, and white adipose tissues during chronic β3-Adrenergic receptor activation

Emilio P. Mottillo^{1,4,*}, Priya Balasubramanian^{1,*}, Yun-Hee Lee¹, Changren Weng¹, Erin E. Kershaw³, and James G. Granneman^{1,2}

¹Center for Integrative Metabolic and Endocrine Research, ²Center for Molecular Medicine and Genetics, Wayne State University School of Medicine, Detroit, Michigan; ³Division of Endocrinology, Department of Medicine, University of Pittsburgh, Pittsburgh, Pennsylvania.

⁴Current Address: Department of Medicine, McMaster University, Hamilton, Ontario, Canada.

*These authors contributed equally to this publication.

Abbreviated title: Lipolysis and lipogenesis are coupled in brown and white fat

Corresponding author:

Downloaded from www.jlr.org by guest, on October 17, 2018

Dr. James Granneman

Center for Integrative Metabolic and Endocrine Research

Wayne State University School of Medicine

550 East Canfield, Detroit, MI 48201

Tel.: 313-577-5629

Fax: 313-577-9469

E-mail: jgranne@med.wayne.edu

Abbreviations

ACC1, acetyl-CoA carboxylase 1; ACLY, ATP-citrate lyase; ATGL, adipose triacylglycerol lipase; BA, brown adipocyte; BAT, brown adipose tissue; β3-AR, β3-adrenergic receptor; CL, CL 316,243; Cox8b, cytochrome c oxidase subunit VIIIb; FASN, fatty acid synthase; FFA, free fatty acid; gWAT, gonadal white adipose tissue; iWAT, inguinal white adipose tissue; LCAD, long chain acyl-CoA dehydrogenase; MCAD, medium-chain acyl-CoA dehydrogenase; PPAR, peroxisome proliferator-activated receptor; qPCR, quantitative polymerase chain reaction; TG, triglyceride; UCP1, uncoupling protein 1, WAT, white adipose tissue



,

Abstract

Chronic activation of \(\beta \)-adrenergic receptors (\(\beta \)-ARs) expands the catabolic activity of both brown adipose tissue (BAT) and white adipose tissue (WAT) by engaging UCP1dependent and UCP1 independent processes. The present work examined de novo lipogenesis (DNL) and triglyceride (TG)/glycerol dynamics in classic brown, subcutaneous 'beige', and classic WAT during sustained β3-AR activation by CL 316,243 (CL), and also addressed the contribution of TG hydrolysis to these dynamics. CL treatment for 7 days dramatically increased DNL and TG turnover similarly in all adipose depots, despite great differences in UCP1 abundance. Increased lipid turnover was accompanied by the simultaneous upregulation of genes involved in both fatty acid synthesis, glycerol metabolism, and fatty acid oxidation. Inducible, adipocyte-specific deletion of adipose triglyceride lipase (ATGL), the rate limiting enzyme for lipolysis, demonstrates that TG hydrolysis is required for CL-induced increases in DNL, TG turnover, and mitochondrial electron transport in all depots. Interestingly, the effect of ATGL deletion on induction of specific genes involved in fatty acid oxidation and synthesis varied among fat depots. Overall, these studies indicate that fatty acid synthesis and oxidation are tightly coupled in adipose tissues during chronic adrenergic activation, and this effect critically depends on the activity of adipocyte ATGL.

Downloaded from www.jlr.org by guest, on October 17, 2018

Supplementary key words: beige, adipose triglyceride lipase (ATGL), UCP1, lipid synthesis, adiponectin-CreERT2

Introduction

Classic interscapular brown adipose tissue (BAT) is a thermogenic organ that has a high capacity for uncoupled oxidative metabolism (1). In contrast, white adipose tissue (WAT) has low oxidative capacity since its main function under normal conditions is to store excess energy as triglycerides (TGs). However, chronic stimulation by β 3-adrenergic receptors (β 3-ARs) expands the oxidative capacity of WAT and converts it into a tissue resembling BAT. This phenomenon has been termed "browning" of white fat (2-4), and is marked by increased expression of oxidative genes, induction of UCP1 protein, and activation of oxidative metabolism (5). Importantly, lipolysis plays a central role in the catabolic activity of BAT and WAT. Acutely, mobilized fatty acids uncouple oxidative phosphorylation, and provide fuel that supports both coupled and uncoupled respiration (6). Lipolysis also provides ligands for peroxisome proliferator activated receptor (PPAR) α , which plays a central role in catabolic remodeling of WAT by upregulating oxidative metabolism and limiting fatty acid-induced inflammation (7, 8). Indeed, several recent studies have demonstrated the importance of lipolysis in providing ligands for activation of PPAR target genes in BAT (9, 10), heart (11), liver (12, 13), and pancreatic β -cells (14).

Although activation of β3-ARs can similarly increase oxidative metabolism in BAT and WAT, the increase in UCP1 protein varies greatly among the various adipose tissue depots (2). Adrenergic activation dramatically upregulates UCP1 expression in inguinal white (or "beige") adipose tissue (iWAT), where basal levels are very low; however, the absolute levels of UCP1 protein expression attained per pad remain far lower than in classic BAT (15, 16). In contrast, gonadal white adipose tissue (gWAT; *i.e,* epididymal white adipose tissue in male mice) exhibits the lowest induction of UCP1, especially in obesity prone strains such as C57Bl/6 (15, 17). In addition, the mechanism by which brown adipocytes (BA) are recruited in WAT also varies: BA in iWAT are derived from pre-existing adipocytes (18), whereas BA in gWAT originate mostly from de novo differentiation of progenitors (2). These differences in UCP1 content and source

of BA suggest that the mechanisms involved in increasing oxidative capacity in different adipose tissue depots might vary as well (6, 19).

Activation of β -ARs by cold stress is known to simultaneously increase fatty acid synthesis and oxidation in classic BAT (20). Whether this occurs in beige or classical WAT depots is not known, nor is it known to what extent the elevation in fatty acid turnover might depend upon UCP1-dependent thermogenesis. Previous studies focused almost exclusively on fatty acid synthesis in BAT following long-term cold adaption (21), and there are no data that assess the acute and chronic effects of direct activation by selective β 3-AR agonists. The purpose of our study was to examine the temporal effects of direct β 3-adrenergic receptor activation on in vivo lipogenesis, TG/glycerol dynamics, and catabolic remodeling. In addition, we examined the role of lipolysis during the dynamics of lipid turnover and gene expression using a new mouse model that allows inducible, adipocyte-specific deletion of ATGL, the rate limiting enzyme for lipolysis.

Downloaded from www.jlr.org by guest, on October 17, 2018

Materials and Methods

Animals. All animal protocols were approved by Institutional Animal Care and Use Committee at Wayne State University. C57Bl/6 (BL6) mice at 7 weeks of age were obtained from The Jackson Laboratory and were fed a standard chow diet (LabDiet, Cat# 5L0D). Mice carrying a LoxP-modified Atgl allele (B6N.129S-Pnpla2^{tm1Eek} mice; herein designated as Atgl-flox mice) on a BL6 background were created as described (22). Transgenic mice harboring tamoxifensensitive Cre recombinase (CreER^{T2}, (23)) under the control of the adiponectin promoter (B6N.129S-Tg(Adipoq-CreER^{T2})^{tm1Jgg} mice; herein designated as Adipoq-CreER^{T2} mice) were generated by standard techniques (24). The transgene was created by inserting CreER^{T2} (23) into the adiponectin translation start site within the bacterial artificial chromosome RP24-69M4 (CHORI.org) using bacterial recombination. Atgl-flox mice were bred with transgenic Adipoq-CreER^{T2} mice to generate control mice (control; homozygous Atgl-flox without Cre, Atgl^{floxflox} -/-)

or an inducible adipose tissue-specific ATGL knockout (iAAKO; homozygous *Atgl*-flox with Cre, *Atgf*^{floxflox} Cre/-). To activate Cre, tamoxifen (20mg/mL) was dissolved in 1mL ethanol, solubilized in 9mL of sunflower oil (filtered 22μM) and given at a dose of 100mg/kg by oral gavage for 5 days in 6-7 week old mice. Experiments were performed on littermate CreER^{T2} negative and CreER^{T2} positive mice ten day after the last treatment of tamoxifen. Mice were genotyped for the floxed allele as described (22). The presence of the Cre-ER^{T2} transgene was determined by PCR using forward primer 5'- TGAAACAGGGGCAATGGTGCG -3' and reverse primer 5'- CGGAATAGAGTATGGGGGGCTCAG -3'. Male or female mice underwent sham surgery (Control; Ctl) or were implanted with mini-osmotic pumps delivering the β3-AR agonist (CL 316,243; CL, 0.75nmol/hr) as previously described (2). Body composition was determined by NMR (EchoMRI) prior to surgeries and on indicated days. Mice were sacrificed in the ad lib fed state on day 1 or 7 of CL treatment and gWAT, iWAT and BAT were collected for RNA, protein, and tracer analysis as described (9, 25). In situ electron transport chain activity was examined in adipose tissue minces by measuring the reduction of 2,3,5-triphenyltetrazolium chloride (TTC, Sigma), as previously described (7).

RNA extraction and gene expression analysis. RNA from adipose tissues were extracted in Trizol (Invitrogen) and then purified with an RNeasy mini kit (Qiagen). The expression pattern of various genes was examined by quantitative PCR (qPCR) analysis, as previously described (8). Briefly, RNA (0.5–1.0 μg) was reverse transcribed into cDNA by using Superscript III (Invitrogen) and oligo(dT) primers. Thirty to 50 ng of cDNA was analyzed in a 20 μl quantitative PCR reaction (ABsolute Blue QPCR SYBR; ThermoScientific) with 80 nM of primers. FASN cDNA was amplified using primers 5'-ACCTCTCCCAGGTGTGTGAC-3' (forward) and 5'-CCTCCCGTACACTCACTCGT-3' (reverse); SCD1 with 5'-AGAGAACTGGAGACGGGAGT-3' (forward) and 5'-GCATCATTAACACCCCGATA-3' (reverse); ACLY with 5'-CTGGTGTATCGGGACCTGT-3' (forward) and 5'-CACAAACACTCCTGCTTCCT-3' (reverse);

and ACC1 with 5'-CTCTGCTAGAGCTGCAGGAT-3' (forward) and 5'-CTGGGAAACTGACACAGGAC-3' (reverse). All other cDNAs were amplified using primers described previously (7). Expression data were normalized to the reference gene peptidyl-prolyl cis-trans isomerase A (PPIA) using the delta-delta CT method (2^{-ΔΔCT}) (26).

Protein isolation and western blot analysis. Adipose tissue extracts were prepared as previously described (8). Resolved proteins were transferred to PVDF, and membranes were immunoblocked for 1 hr at room temperature in 5% powdered skim milk. Western blotting was performed using antibodies against ATGL (27), UCP1 (2), β-tubulin (Invitrogen, #322600), FASN (Cell Signal, #3180), GYK (Abcam, #126599), PEPCK (Abcam, #70358), GAPDH (Santa Cruz, #25778), and MCAD (Santa Cruz, sc-365108) as described (8). Blots were then washed, incubated with a secondary donkey anti-rabbit HRP (Jackson immunological) diluted 1:5000, and visualized with SuperSignal West Dura substrate (Pierce). Digital images were captured to ensure that pixels were not over-saturated using a BioRad Quantity One imaging system.

Measurement of triglyceride and fatty acid concentrations and synthesis using stable isotopes. Mice were enriched with deuterium-labeled water (D_2O) for isotope tracer experiments to approximately 2% 2H by an IP injection of labelled water ($20 \mu l/g$ of body weight of isotonic saline containing > 99% 2H_2O). After injection, mice (n =3-4) were maintained on 5% 2H -labeled drinking water over a 24 hr period on day 1 and day 7 of CL treatment, to maintain a steady-state 2H labelling of body water of \sim 2.75% (25). Blood was collected 2 hrs after IP injection and at the end of labelling to determine label incorporation. Incorporation of 2H_2O into triglyceride and palmitate was measured by the Mouse Metabolic Phenotyping Center (MMPC) of Case Western Reserve University (Cleveland, OH) (28). Briefly, TGs were hydrolyzed with 1 N KOH ethanol at 70 $^{\circ}$ C, and the incorporation of 2H into glycerol and palmitate was determined by mass spectrometry following derivatization (28). Newly-synthesized triglyceride was calculated from the incorporation of 2H into TG-derived glycerol and newly-synthesized palmitate was

determined from the incorporation of ²H into TG-derived palmitate (25). Adipocyte isolations from iWAT and quantification of fatty acids in serum (from *ad lib* fed mice) and cell culture media were performed as previously described (8).

Statistical analysis. Unless stated otherwise, results are expressed as means \pm SEM. Statistical analyses were performed with GraphPad Prism 5 (GraphPad Software) using a Student's t-test, one-way or two-way ANOVA. Planned post-hoc comparisons for one-way or two-way ANOVA were performed using Bonferroni post t-test. Statistical or non-significant changes are as noted (***P < 0.001; **P < 0.01; *P < 0.05; **P < 0.001; **P < 0.01; *P < 0.05; **P < 0.01; *P < 0.05; **P < 0.01 and *P < 0.05; **P < 0.05; **P < 0.01 and *P < 0.05; **P < 0.05;

Results

Sustained \(\beta \)-adrenergic stimulation promotes depot-specific changes in adiposity.

We first examined the effects of CL on total body adiposity and adipose tissue masses over the course of treatment. CL-treated mice lost nearly half of their body fat in the first two days, but fat mass stabilized thereafter (Figure 1A, B) despite ongoing adrenergic stimulation and elevation in metabolic rate (6). As expected, CL treatment reduced total TG in all fat depots after day 1 of treatment (Figure 1C). Remarkably, this reduction was sustained in gWAT but not iWAT or BAT by day 7 of treatment (Figure 1C). Consistent with these results, tissue weight was reduced in gWAT, but not iWAT, BAT, or liver after 7 days of CL treatment (Figure 1D, E). These data suggest that fatty acid mobilization/oxidation exceeds synthesis at the start of CL treatment, but these complementary pathways reach an elevated equilibrium after 7 days.

Chronic \$3-AR activation increases lipid turnover in gWAT, iWAT and BAT.

The observation that TG content of adipose tissues remains constant during sustained adrenergic activation suggested that tissues might upregulate fatty acid synthesis to

compensate for expanded fat oxidation and increased metabolic rate (6, 7). To test this hypothesis, we directly assessed lipid turnover in various fat depots over the 7 day course of CL treatment using the deuterium-labeled water (D₂O) technique (28). ²H enrichment in fatty acids (i.e. palmitate) reflects de novo lipogenesis (DNL), whereas incorporation into glycerol provides a measure of total TG turnover and glyceroneogenesis to supports fatty acid esterification (i.e. "new triglyceride"). Rates of DNL were similar across fat pads of untreated control mice (Figure 2A), whereas basal incorporation of ²H-label into new TGs was much higher in BAT compared to iWAT or gWAT (Figure 2B). After 1 day of CL treatment, DNL was unchanged, whereas glycerol turnover in new TGs was dramatically increased in all fat depots (Figure 2A vs. 2B). After 7 days of CL treatment, both DNL and glycerol turnover were elevated in all fat pads, with the highest turnover in BAT (Figure 2A vs. 2B). However, the increase in glycerol turnover was comparable at day 1 and 7 of CL treatment. These data indicate CL induces a futile substrate cycle of lipolysis and re-esterification without a net increase in lipogenesis after 1 day of treatment, whereas lipid turnover is drastically elevated in all fat depots by 7 days.

Chronic β 3-AR activation simultaneously increases the expression of genes and proteins involved in lipid oxidation and synthesis.

Analysis of lipid turnover suggested that CL treatment produces temporally distinct changes in fatty acid catabolism, synthesis, and glycerol metabolism. To gain deeper insight into this regulation we evaluated the mRNA (Table 1) and protein expression (Figure 3) of key catabolic and synthetic genes across the various fat depots over the course of CL treatment. As expected, basal expression of genes involved in fatty acid catabolism and thermogenesis were far greater in BAT compared to WAT depots. Interestingly, CL treatment did not significantly upregulate these genes in BAT and, in fact, lowered expression of cytochrome c oxidase subunit VIIIb (Cox8b). In addition, CL treatment greatly upregulated expression of long-chain acyl-CoA dehydrogenase (LCAD) and Cox8b in the WAT depots, and while CL increased

expression of UCP1, particularly in iWAT, the levels achieved were less than 5% of BAT. Immunoblot analysis confirmed the strong upregulation of medium chain acyl-CoA dehydrogenase that was largely independent of UCP1 levels in the WAT depots (Figure 3). Basal proteins of MCAD and UCP1 in BAT were greater than that of WAT and were further upregulated by 7 days of CL treatment (Figure 3C). Analysis of genes involved in de novo synthesis (fatty acid synthase (FASN), steryl-CoA desaturase (SCD1) and ATP-citrate lyase (ACLY), acetyl-CoA carboxylase 1 (ACC1)), revealed a somewhat different pattern with BAT and gWAT showing initial suppression, then overexpression by day 7 (Table 1). In contrast, 1 day CL initially suppressed expression of lipogenic genes in iWAT, which then recovered to control levels by day 7 (Table 1). Despite the different induction pattern of DNL genes in the fat pads, 7 days of CL greatly elevated protein levels of FASN in all the depots (Figure 3). Glycerol kinase (GYK), which generates α-glycerol-3 phosphate for fatty acid esterification, was generally lower in WAT compared to BAT. CL treatment rapidly induced expression of GYK in WAT to levels that exceeded those observed in BAT (Table 1). Interestingly, levels of GYK mRNA declined by 7 days, yet GYK protein remained elevated (shown below). Phosphoenolpyruvate carboxykinase (PEPCK) is a key enzyme of glyceroneogenesis, and its pattern of expression was highly similar to lipogenic genes that were initially suppressed, then recovered, or were overexpressed by 7 days (see below, as well). Thus chronic β3-AR activation simultaneously increases the expression of genes involved in lipid catabolism and synthesis in the adipose depots.

Adipocyte ATGL is required for loss of adiposity by chronic CL treatment.

The compensatory changes in lipid synthesis and glycerol turnover following CL treatment suggest that increased lipid flux and TG hydrolysis (lipolysis) might be required for CL-induced body fat loss. To address this question, we generated mice with inducible, adipocyte-specific deletion of ATGL, the rate limiting enzyme for lipolysis (29). Treatment of

mice with tamoxifen effectively deleted ATGL in all adipose tissue depots of mice carrying CreER^{T2} allele (iAAKO, inducible ATGL knockout), but not in tamoxifen-treated mice lacking CreER^{T2} (Control; Figure 4A). Induced deletion of ATGL abolished isoproterenol (a general β-AR receptor agonist) and CL-stimulated lipolysis in isolated adipocytes (Figure 4B), indicating that the defect in lipolysis is not specific to CL. In addition, CL-induced elevation in serum fatty acids was also abolished in iAAKO mice (Figure 4C). Control and iAAKO mice were then treated for 7 days with CL to examine the effect of lipolysis on adiposity. As expected, control mice lost a significant amount of body fat mass in response to 7 days of CL treatment, whereas iAAKO were resistant to CL-induced loss of fat mass (Figure 4D). This difference was primarily due to a resistance to the CL-inducedreduction of gWAT mass in combination with an increase in iWAT and BAT mass (Figure 4E, F; &&& denotes an overall ATGL effect). These data demonstrate that adipocyte ATGL action is required for the loss of body fat mass by chronic CL treatment.

Adipocyte ATGL is required for enhanced lipid turnover and induction of proteins involved in DNL and TG turnover.

To further assess the role of TG hydrolysis during chronic β 3-AR activation, we next determined the effects of inducible ATGL knockout on lipid turnover in response to 7 days of CL treatment. Inducible adipocyte knockout of ATGL did not affect basal rates of DNL in WAT or BAT (Figure 5A). Basal incorporation of new glycerol into TG also was not affected by loss of ATGL in WAT, but was reduced by greater than 50% in BAT (Figure 5B). As expected, 7 days of CL treatment greatly increased the de novo synthesis of palmitate and glycerol in gWAT, iWAT, and BAT of control mice, and these effects were absent in iAAKO (Figure 5A,B). These data confirm that the increase in lipid turnover by chronic β 3-AR activation requires adipocyte TG hydrolysis.

We next explored the mechanism by which loss of ATGL in adipocytes abolishes CL-induced lipid turnover by measuring proteins involved in fatty acid synthesis and glycerol turnover. Inducible deletion of ATGL in adipocytes had no effect on basal levels of FASN in gWAT or BAT, whereas overall levels of FASN were slightly lower in iWAT (Figure 6A).

Importantly, ATGL knockout prevented induction of FASN by chronic CL treatment in gWAT and BAT. Likewise, CL-mediated induction of PEPCK protein was abolished in gWAT and iWAT (Figure 6B). Furthermore, the high levels of PEPCK observed in BAT were reduced by more than 90% by ATGL knockout, and these low levels were completely unresponsive to induction by CL. Finally, ATGL knockout also prevented upregulation of GYK protein by CL in gWAT and BAT (Figure 6C). Surprisingly, ATGL knockout did not prevent the strong induction of GYK in iWAT. These results suggest that ATGL promotes lipid turnover by regulating the induction of proteins involved in DNL and TG turnover.

Adipocyte ATGL is required for the increase in tissue respiration, but differentially regulates the induction of markers of lipid oxidation in gWAT, iWAT and BAT.

Because ATGL has been shown to influence mitochondrial function (9-11), we next sought to determine whether ATGL action was required for CL-mediated effects on mitochondrial respiration. To do so, we examined mitochondrial electron transport chain activity in situ using the redox dye TTC (5, 7), and on oxidative gene expression by qPCR and western blot in both control and iAAKO mice treated with CL. Inducible ATGL deletion reduced basal electron transport activity in BAT, and completely eliminated CL-mediated upregulation of electron chain activity in all fat depots (Figure 7A). LCAD and UCP1 mRNA were similarly induced in the gWAT of control and iAAKO mice (Figure 7B). Deletion of ATGL reduced the induction of LCAD and UCP1 mRNA by CL in iWAT, and reduced overall mRNA expression in BAT (Figure 7B). Immunoblot analysis of the adipose depots indicated that 7 days of CL increased the expression of MCAD in the WAT depots of control mice; however, the induction of

MCAD was sustained in gWAT, but not in iWAT of iAAKO mice (Figure 7C, D). Protein Levels of MCAD trended lower in BAT of iAAKO mice, but this did not reach statistical significance. UCP1 protein was similarly induced by CL in iWAT of iAAKO mice, however the induction was highly variable (Figure 7C, E). There was an overall effect of CL on UCP1 protein levels in BAT (p>0.05), which tended to be lower in iAAKO mice. Protein levels of UCP1 were barely detectable in gWAT of mice and thus were not quantified. Overall, these results indicate that ATGL is required for increased mitochondrial respiration induced by chronic CL treatment in the adipose tissue depots.

Discussion

This study examined the relationship between lipid hydrolysis, oxidation, and de novo synthesis in adipose tissue. The most salient feature of β 3-AR activation is the stimulation of lipolysis which promotes fatty acid oxidation and uncoupling. We found that chronic stimulation enhanced lipid turnover in gWAT, iWAT and BAT depots that differ vastly in their UCP1 content. Mechanistically, chronic β 3-AR stimulation simultaneously increased the expression of genes and proteins involved in lipid catabolism and synthesis. Adipocyte deletion of ATGL abolished the increase in lipid turnover by β 3-AR activation; however, the induction of genes and protein involved in lipid oxidation and turnover were regulated by ATGL in a depot specific manner. These finding suggest that lipid oxidation and synthesis are functionally linked to hydrolysis, but the mechanisms of gene regulation (*i.e.* ATGL dependent and PKA dependent pathways) are likely to differ among the adipose depots (Figure 8).

Downloaded from www.jlr.org by guest, on October 17, 2018

Lipolysis and lipogenesis are typically viewed as independent, opposing pathways.

Indeed, CL treatment uniformly suppressed DNL in the first day of treatment. This initial suppression of DNL is likely due to the inundation of systemic FFAs, as previously reported (5).

Accordingly, one day of CL treatment strongly upregulated TG re-esterification, as indicated by

the large enrichment of labeled glycerol in TG and the upregulation of GYK expression, although PEPCK mRNA was not upregulated at this time. By seven days of treatment, DNL was similarly expanded in all fat pads examined. We note that the turnover of lipid, induction of oxidative genes, and expanded mitochondrial electron transport activity were largely independent of differences in UCP1 expression. While the current experimental design did not allow us to determine the exact site of DNL *per se* (i.e. liver vs. fat), the upregulation of lipogenic enzymes in adipose tissues strongly suggests that adipocytes are the major site of DNL. In agreement, cold exposure elevates fatty acid synthesis in BAT while reducing synthesis in liver (21). Interestingly, plasma lipoprotein clearance plays a larger role in BAT lipid metabolism than in WAT (30, 31), and could be important in determining the relative contribution of DNL to the different adipose tissue depots (32).

Fatty acids are both necessary and sufficient to drive thermogenesis by directly activating UCP1 (33) and by providing fuel for high rates of oxidative metabolism. Accordingly, fat is preferentially oxidized over carbohydrate and protein during cold exposure in rodents (34), and the increase in DNL would allow lipid supply to be matched with greater rates of lipid oxidation. In contrast to BAT, gWAT normally has low oxidative capacity and is largely considered a site for the storage rather than oxidation of triglycerides. It is thus surprising that adrenergic activation produced the greatest increases in lipogenesis in gWAT, as measured by gene expression and lipid flux. Futile cycling is one likely mechanism increasing oxidative metabolism in the absence of UCP1 (6, 19). Thus, the continuous cycle of triglyceride hydrolysis coupled to re-synthesis that requires large amounts of ATP could be an important mechanism in increasing metabolic rate in WAT.

The relative physiological contribution of various adipose depots to overall thermogenesis is a matter of debate (16, 36). Our results indicate that lipid dynamics are similar across BAT and WAT in mice treated with the β3-AR agonist for seven days. To the extent that

synthesis is matched by oxidation, the current results suggest that each fat pad is an important contributor to overall oxidative metabolism. In agreement, WAT is required for the full thermogenic response to CL (37). With the recent emphasis on beige or brite fat and its proposed similarity to brown fat in humans (38), strategies that increase lipid turnover in these tissues might contribute significantly to improvements in whole body metabolism in rodents and humans (39).

Recent work demonstrates that adipose tissue DNL is important in regulating glucose homeostasis (40). While glucose is thought to be the major precursor for DNL when mice are fed a diet high in carbohydrate, as much as one third of TG/glycerol can be derived from non-glucose sources (i.e., glyceronegenesis via PEPCK) (28). We found that GYK mRNA was greatly elevated at day 1 of CL treatment, while the expression of PEPCK was initially suppressed, suggesting GYK is more important for fatty acid cycling, whereas PEPCK plays a larger role in coupling DNL to TG synthesis. The induction of PEPCK protein was highly influenced by ATGL acticity in all fat depots. Surprisingly, however, the increase in GYK protein by chronic CL treatment was dependent upon ATGL in gWAT and BAT, but not iWAT. PEPCK and GYK are both PPAR and cAMP response element targets, which may explain their differential regulation among the adipose tissue depots (see below).

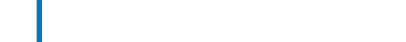
Recent work from various labs indicates that lipolysis also contributes to cellular signaling events (10, 11, 14, 41) by providing ligands for PPAR α and δ which, in turn serve to match lipid oxidation with supply (9). We therefore reasoned that lipolysis was also driving the increase in lipogenesis and oxidation, and tested this by deleting ATGL in adipose tissue of adult mice using an inducible model. Previous studies demonstrated that conditional knockout of ATGL in adipocytes results in defective lipolysis, increase in body fat mass, and a reduction in fatty acid oxidation and PPAR α target genes (10, 42). In our study inducible deletion of ATGL in adipocytes also abolished lipolysis and increased iWAT and BAT depots weights, and

eliminated the increase in mitochondrial respiration by CL. However, in our model, the induction of MCAD and UCP1 were unaffected in gWAT, and minimally reduced in iWAT, suggesting that the primary defect in respiration in the WAT depots is in the substrate supply. MCAD and UCP1 are direct targets of PKA signaling (43), which appears to be preserved in the WAT depots and also when ATGL is acutely deleted in adults (present result), but not when chronically deleted during development (9). We observed that lipolysis was required for greater lipid synthesis in the brown and white fat depots, which links lipid hydrolysis to oxidation and synthesis and implies that distinct pools of lipids are channeled towards synthesis (44) and oxidation (45). In agreement with our observations, overexpression of ATGL enhanced incorporation of palmitate into TG (46). Altogether, these results indicate that lipolysis drives the increase in oxidation and is required for coupling to enhanced synthesis across the adipose tissue depots.

It is attractive to speculate that products of lipid metabolism might be sensed to upregulate lipogenesis to match with catabolic activity. DNL produces lipid species that are biologically active and are functionally distinct from dietary lipids (47, 48), as is the case with the production of a FASN-dependent PPAR γ ligand in adipose tissue (49). In this regard, PPAR δ activation in liver generates ligands that activate skeletal muscle PPAR α , thereby matching hepatic lipogenesis with muscle lipid oxidation (50). Whether such crosstalk occurs among or within fat depots requires additional exploration. At the molecular level, PGC1 α and β (51), carbohydrate-responsive-element-binding protein (52), sterol regulatory element-binding protein-1 (53) could be involved in detecting signals to enhance lipid synthesis. Further understanding the mechanisms by which lipolysis elevates DNL to match with greater fat oxidation might prove useful in targeting pathways which improve adipose tissue function.

Acknowledgements

This work was supported by National Institutes of Health grants DK092741, DK076229 and DK062292 to J.G.G; DK090166 and Howard Hughes Medical Institute Physician-Scientist Early Career Award to E.E.K.; and grant U24 DK76174 to MMPC of Case Western Reserve University. E.P.M. was supported by a CIHR Doctoral Research Award MDR-214349. The author would like to thank Drs. Michelle Puchowicz and Colleen Croniger at the MMPC for helpful discussions.



References

- 1. Feldmann, H. M., V. Golozoubova, B. Cannon, and J. Nedergaard. 2009. UCP1 ablation induces obesity and abolishes diet-induced thermogenesis in mice exempt from thermal stress by living at thermoneutrality. *Cell Metab* **9**: 203-209.
- 2. Lee, Y.-H., Anelia P. Petkova, Emilio P. Mottillo, and James G. Granneman. 2012. In Vivo Identification of Bipotential Adipocyte Progenitors Recruited by β3-Adrenoceptor Activation and High-Fat Feeding. *Cell metabolism* **15**: 480-491.
- 3. Seale, P., H. M. Conroe, J. Estall, S. Kajimura, A. Frontini, J. Ishibashi, P. Cohen, S. Cinti, and B. M. Spiegelman. 2011. Prdm16 determines the thermogenic program of subcutaneous white adipose tissue in mice. *The Journal of clinical investigation* **121**: 96-105.
- 4. Lee, Y.-H., E. P. Mottillo, and J. G. Granneman. 2014. Adipose tissue plasticity from WAT to BAT and in between. *Biochimica et Biophysica Acta (BBA) Molecular Basis of Disease* **1842**: 358-369.
- 5. Granneman, J. G., P. Li, Z. Zhu, and Y. Lu. 2005. Metabolic and cellular plasticity in white adipose tissue I: effects of beta3-adrenergic receptor activation. *American journal of physiology* **289**: E608-616.
- 6. Granneman, J. G., M. Burnazi, Z. Zhu, and L. A. Schwamb. 2003. White adipose tissue contributes to UCP1-independent thermogenesis. *American journal of physiology* **285**: E1230-1236.
- 7. Li, P., Z. Zhu, Y. Lu, and J. G. Granneman. 2005. Metabolic and cellular plasticity in white adipose tissue II: role of peroxisome proliferator-activated receptor-alpha. *American journal of physiology* **289**: E617-626.
- 8. Mottillo, E. P., X. J. Shen, and J. G. Granneman. 2007. Role of hormone-sensitive lipase in beta-adrenergic remodeling of white adipose tissue. *American journal of physiology* **293**: E1188-1197.

Downloaded from www.jlr.org by guest, on October 17, 2018

- 9. Mottillo, E. P., A. E. Bloch, T. Leff, and J. G. Granneman. 2012. Lipolytic Products Activate Peroxisome Proliferator-activated Receptor (PPAR) α and δ in Brown Adipocytes to Match Fatty Acid Oxidation with Supply. *Journal of Biological Chemistry* **287**: 25038-25048.
- 10. Ahmadian, M., M. J. Abbott, T. Tang, C. S. Hudak, Y. Kim, M. Bruss, M. K. Hellerstein, H. Y. Lee, V. T. Samuel, G. I. Shulman, Y. Wang, R. E. Duncan, C. Kang, and H. S. Sul. 2011. Desnutrin/ATGL is regulated by AMPK and is required for a brown adipose phenotype. *Cell metabolism* **13**: 739-748.
- 11. Haemmerle, G., T. Moustafa, G. Woelkart, S. Buttner, A. Schmidt, T. van de Weijer, M. Hesselink, D. Jaeger, P. C. Kienesberger, K. Zierler, R. Schreiber, T. Eichmann, D. Kolb, P. Kotzbeck, M. Schweiger, M. Kumari, S. Eder, G. Schoiswohl, N. Wongsiriroj, N. M. Pollak, F. P. Radner, K. Preiss-Landl, T. Kolbe, T. Rulicke, B. Pieske, M. Trauner, A. Lass, R. Zimmermann, G. Hoefler, S. Cinti, E. E. Kershaw, P. Schrauwen, F. Madeo, B. Mayer, and R. Zechner. 2011. ATGL-mediated fat catabolism regulates cardiac mitochondrial function via PPAR-alpha and PGC-1. *Nature medicine* 17: 1076-1085.
- 12. Ong, K. T., M. T. Mashek, S. Y. Bu, A. S. Greenberg, and D. G. Mashek. 2011. Adipose triglyceride lipase is a major hepatic lipase that regulates triacylglycerol turnover and fatty acid signaling and partitioning. *Hepatology (Baltimore, Md.)* **53**: 116-126.
- 13. Sapiro, J. M., M. T. Mashek, A. S. Greenberg, and D. G. Mashek. 2009. Hepatic triacylglycerol hydrolysis regulates peroxisome proliferator-activated receptor alpha activity. *J Lipid Res* **50**: 1621-1629.
- 14. Tang, T., M. J. Abbott, M. Ahmadian, A. B. Lopes, Y. Wang, and H. S. Sul. 2013. Desnutrin/ATGL activates PPARdelta to promote mitochondrial function for insulin secretion in islet beta cells. *Cell metabolism* **18**: 883-895.

- 15. Xue, B., A. Coulter, J. S. Rim, R. A. Koza, and L. P. Kozak. 2005. Transcriptional synergy and the regulation of Ucp1 during brown adipocyte induction in white fat depots. *Mol Cell Biol* **25**: 8311-8322.
- 16. Shabalina, I. G., N. Petrovic, J. M. de Jong, A. V. Kalinovich, B. Cannon, and J. Nedergaard. 2013. UCP1 in Brite/Beige Adipose Tissue Mitochondria Is Functionally Thermogenic. *Cell reports* **5**: 1196-1203.
- 17. Almind, K., M. Manieri, W. I. Sivitz, S. Cinti, and C. R. Kahn. 2007. Ectopic brown adipose tissue in muscle provides a mechanism for differences in risk of metabolic syndrome in mice. *Proc Natl Acad Sci U S A* **104**: 2366-2371.
- 18. Rosenwald, M., A. Perdikari, T. Rulicke, and C. Wolfrum. 2013. Bi-directional interconversion of brite and white adipocytes. *Nature cell biology* **15**: 659-667.
- 19. Ukropec, J., R. P. Anunciado, Y. Ravussin, M. W. Hulver, and L. P. Kozak. 2006. UCP1-independent thermogenesis in white adipose tissue of cold-acclimated Ucp1-/- mice. *J Biol Chem* **281**: 31894-31908.
- 20. Yu, X. X., D. A. Lewin, W. Forrest, and S. H. Adams. 2002. Cold elicits the simultaneous induction of fatty acid synthesis and beta-oxidation in murine brown adipose tissue: prediction from differential gene expression and confirmation in vivo. *FASEB journal : official publication of the Federation of American Societies for Experimental Biology* **16**: 155-168.
- 21. Trayhurn, P. 1981. Fatty acid synthesis in mouse brown adipose tissue. The influence of environmental temperature on the proportion of whole-body fatty acid synthesis in brown adipose tissue and the liver. *Biochimica et biophysica acta* **664**: 549-560.
- 22. Sitnick, M. T., M. K. Basantani, L. Cai, G. Schoiswohl, C. F. Yazbeck, G. Distefano, V. Ritov, J. P. DeLany, R. Schreiber, D. B. Stolz, N. P. Gardner, P. C. Kienesberger, T. Pulinilkunnil, R. Zechner, B. H. Goodpaster, P. Coen, and E. E. Kershaw. 2013. Skeletal Muscle Triacylglycerol Hydrolysis Does Not Influence Metabolic Complications of Obesity. *Diabetes* 62: 3350-3361.

Downloaded from www.jir.org by guest, on October 17, 2018

- 23. Eguchi, J., X. Wang, S. Yu, Erin E. Kershaw, Patricia C. Chiu, J. Dushay, Jennifer L. Estall, U. Klein, E. Maratos-Flier, and Evan D. Rosen. 2011. Transcriptional Control of Adipose Lipid Handling by IRF4. *Cell metabolism* **13**: 249-259.
- 24. Seibler, J., B. Zevnik, B. Küter-Luks, S. Andreas, H. Kern, T. Hennek, A. Rode, C. Heimann, N. Faust, G. Kauselmann, M. Schoor, R. Jaenisch, K. Rajewsky, R. Kühn, and F. Schwenk. 2003. Rapid generation of inducible mouse mutants. *Nucleic Acids Research* **31**: e12.
- 25. Brunengraber, D. Z., B. J. McCabe, T. Kasumov, J. C. Alexander, V. Chandramouli, and S. F. Previs. 2003. Influence of diet on the modeling of adipose tissue triglycerides during growth. *American journal of physiology* **285**: E917-925.
- 26. Livak, K. J., and T. D. Schmittgen. 2001. Analysis of Relative Gene Expression Data Using Real-Time Quantitative PCR and the 2-[Delta][Delta]CT Method. *Methods* **25**: 402-408.
- 27. Granneman, J. G., H.-P. H. Moore, E. P. Mottillo, Z. Zhu, and L. Zhou. 2011. Interactions of Perilipin-5 (Plin5) with Adipose Triglyceride Lipase. *Journal of Biological Chemistry* **286**: 5126-5135.
- 28. Bederman, I. R., S. Foy, V. Chandramouli, J. C. Alexander, and S. F. Previs. 2009. Triglyceride synthesis in epididymal adipose tissue: contribution of glucose and non-glucose carbon sources. *J Biol Chem* **284**: 6101-6108.
- 29. Zimmermann, R., A. Lass, G. Haemmerle, and R. Zechner. 2009. Fate of fat: the role of adipose triglyceride lipase in lipolysis. *Biochimica et biophysica acta* **1791**: 494-500.
- 30. Garcia-Arcos, I., Y. Hiyama, K. Drosatos, K. G. Bharadwaj, Y. Hu, N. H. Son, S. M. O'Byrne, C. L. Chang, R. J. Deckelbaum, M. Takahashi, M. Westerterp, J. C. Obunike, H. Jiang, H. Yagyu, W. S. Blaner, and I. J. Goldberg. 2013. Adipose-specific lipoprotein lipase deficiency more profoundly affects brown than white fat biology. *J Biol Chem* **288**: 14046-14058.
- 31. Bartelt, A., O. T. Bruns, R. Reimer, H. Hohenberg, H. Ittrich, K. Peldschus, M. G. Kaul, U. I. Tromsdorf, H. Weller, C. Waurisch, A. Eychmuller, P. L. Gordts, F. Rinninger, K.

- 32. Bartelt, A., C. Weigelt, M. L. Cherradi, A. Niemeier, K. Todter, J. Heeren, and L. Scheja. 2013. Effects of adipocyte lipoprotein lipase on de novo lipogenesis and white adipose tissue browning. *Biochimica et biophysica acta* **1831**: 934-942.
- 33. Nicholls, D. G., and E. Rial. 1999. A history of the first uncoupling protein, UCP1. *Journal of bioenergetics and biomembranes* **31**: 399-406.
- 34. Vaillancourt, E., F. Haman, and J. M. Weber. 2009. Fuel selection in Wistar rats exposed to cold: shivering thermogenesis diverts fatty acids from re-esterification to oxidation. *The Journal of physiology* **587**: 4349-4359.
- 35. Van den Brandt, P. A., and P. Trayhurn. 1981. Suppression of fatty acids synthesis in brown adipose tissue of mice fed diets rich in long chain fatty acids. *Biochimica et biophysica acta* **665**: 602-607.
- 36. Cohen, P., J. D. Levy, Y. Zhang, A. Frontini, D. P. Kolodin, K. J. Svensson, J. C. Lo, X. Zeng, L. Ye, M. J. Khandekar, J. Wu, S. C. Gunawardana, A. S. Banks, J. P. Camporez, M. J. Jurczak, S. Kajimura, D. W. Piston, D. Mathis, S. Cinti, G. I. Shulman, P. Seale, and B. M. Spiegelman. 2014. Ablation of PRDM16 and Beige Adipose Causes Metabolic Dysfunction and a Subcutaneous to Visceral Fat Switch. *Cell* **156**: 304-316.
- 37. Grujic, D., V. S. Susulic, M. E. Harper, J. Himms-Hagen, B. A. Cunningham, B. E. Corkey, and B. B. Lowell. 1997. Beta3-adrenergic receptors on white and brown adipocytes mediate beta3-selective agonist-induced effects on energy expenditure, insulin secretion, and food intake. A study using transgenic and gene knockout mice. *J Biol Chem* **272**: 17686-17693.
- 38. Wu, J., P. Bostrom, L. M. Sparks, L. Ye, J. H. Choi, A. H. Giang, M. Khandekar, K. A. Virtanen, P. Nuutila, G. Schaart, K. Huang, H. Tu, W. D. van Marken Lichtenbelt, J. Hoeks, S. Enerback, P. Schrauwen, and B. M. Spiegelman. 2012. Beige adipocytes are a distinct type of thermogenic fat cell in mouse and human. *Cell* **150**: 366-376.
- 39. Vallerand, A. L., J. Zamecnik, P. J. Jones, and I. Jacobs. 1999. Cold stress increases lipolysis, FFA Ra and TG/FFA cycling in humans. *Aviation, space, and environmental medicine* **70**: 42-50.

Downloaded from www.jir.org by guest, on October 17, 2018

- 40. Marcelino, H., C. Veyrat-Durebex, S. Summermatter, D. Sarafian, J. Miles-Chan, D. Arsenijevic, F. Zani, J. P. Montani, J. Seydoux, G. Solinas, F. Rohner-Jeanrenaud, and A. G. Dulloo. 2013. A role for adipose tissue de novo lipogenesis in glucose homeostasis during catch-up growth: a Randle cycle favoring fat storage. *Diabetes* **62**: 362-372.
- 41. Zechner, R., R. Zimmermann, T. O. Eichmann, S. D. Kohlwein, G. Haemmerle, A. Lass, and F. Madeo. 2012. FAT SIGNALS--lipases and lipolysis in lipid metabolism and signaling. *Cell Metab* **15**: 279-291.
- 42. Wu, J. W., S. P. Wang, S. Casavant, A. Moreau, G. S. Yang, and G. A. Mitchell. 2012. Fasting energy homeostasis in mice with adipose deficiency of desnutrin/adipose triglyceride lipase. *Endocrinology* **153**: 2198-2207.
- 43. Wang, B., L. Zhu, S. Sui, C. Sun, H. Jiang, and D. Ren. 2014. Cilostazol induces mitochondrial fatty acid beta-oxidation in C2C12 myotubes. *Biochemical and biophysical research communications* **447**: 441-445.
- 44. Bu, S. Y., and D. G. Mashek. 2010. Hepatic long-chain acyl-CoA synthetase 5 mediates fatty acid channeling between anabolic and catabolic pathways. *J Lipid Res* **51**: 3270-3280.
- 45. Banke, N. H., A. R. Wende, T. C. Leone, J. M. O'Donnell, E. D. Abel, D. P. Kelly, and E. D. Lewandowski. 2010. Preferential oxidation of triacylglyceride-derived fatty acids in heart is augmented by the nuclear receptor PPARalpha. *Circulation research* **107**: 233-241.
- 46. Ahmadian, M., R. E. Duncan, K. A. Varady, D. Frasson, M. K. Hellerstein, A. L. Birkenfeld, V. T. Samuel, G. I. Shulman, Y. Wang, C. Kang, and H. S. Sul. 2009. Adipose overexpression of desnutrin promotes fatty acid use and attenuates diet-induced obesity. *Diabetes* **58**: 855-866.

- 47. Cao, H., K. Gerhold, J. R. Mayers, M. M. Wiest, S. M. Watkins, and G. S. Hotamisligil. 2008. Identification of a lipokine, a lipid hormone linking adipose tissue to systemic metabolism. *Cell* **134**: 933-944.
- 48. Chakravarthy, M. V., I. J. Lodhi, L. Yin, R. R. Malapaka, H. E. Xu, J. Turk, and C. F. Semenkovich. 2009. Identification of a physiologically relevant endogenous ligand for PPARalpha in liver. *Cell* **138**: 476-488.
- 49. Lodhi, I. J., L. Yin, A. P. Jensen-Urstad, K. Funai, T. Coleman, J. H. Baird, M. K. El Ramahi, B. Razani, H. Song, F. Fu-Hsu, J. Turk, and C. F. Semenkovich. 2012. Inhibiting adipose tissue lipogenesis reprograms thermogenesis and PPARgamma activation to decrease diet-induced obesity. *Cell metabolism* **16**: 189-201.
- 50. Liu, S., J. D. Brown, K. J. Stanya, E. Homan, M. Leidl, K. Inouye, P. Bhargava, M. R. Gangl, L. Dai, B. Hatano, G. S. Hotamisligil, A. Saghatelian, J. Plutzky, and C. H. Lee. 2013. A diurnal serum lipid integrates hepatic lipogenesis and peripheral fatty acid use. *Nature* **502**: 550-554.
- 51. Espinoza, D. O., L. G. Boros, S. Crunkhorn, H. Gami, and M. E. Patti. 2010. Dual modulation of both lipid oxidation and synthesis by peroxisome proliferator-activated receptorgamma coactivator-1alpha and -1beta in cultured myotubes. *FASEB journal : official publication of the Federation of American Societies for Experimental Biology* **24**: 1003-1014.
- 52. Herman, M. A., O. D. Peroni, J. Villoria, M. R. Schon, N. A. Abumrad, M. Bluher, S. Klein, and B. B. Kahn. 2012. A novel ChREBP isoform in adipose tissue regulates systemic glucose metabolism. *Nature* **484**: 333-338.
- 53. Takahashi, Y., A. Shinoda, N. Furuya, E. Harada, N. Arimura, I. Ichi, Y. Fujiwara, J. Inoue, and R. Sato. 2013. Perilipin-mediated lipid droplet formation in adipocytes promotes sterol regulatory element-binding protein-1 processing and triacylglyceride accumulation. *PloS one* **8**: e64605.

Figure and Table Legends

Table 1: Chronic \(\beta \)-AR activation increases expression of genes involved in oxidation (LCAD, Cox8b and UCP1), lipogenesis (FASN, SCD1, ACLY and ACC1), and glycerol turn over (Gyk and PEPCK) in adipose tissue depots. Mice (male, 8 weeks of age, n=4) were treated with the β3-AR agonist (CL) for 7 days and adipose tissue depots (gWAT, iWAT, BAT) were collected after day one of CL treatment (1D CL) or on 7 days of treatment (7D CL) and the mRNA expression for indicated genes was measured by qPCR. Data were analyzed by one-way ANOVA. * denotes significant difference from all the other groups (***P < 0.001; **P < 0.01; *P < 0.05), # denotes difference between control and 1D CL (###P < 0.001; ##P < 0.01; *P < 0.05), * denotes difference between control and 7D CL (*&*P < 0.001; *&*P < 0.01); $^{\&}P < 0.05$) and $^{\$}$ denotes difference between 1D and 7D CL ($^{\$\$}P < 0.01$ and $^{\$}P < 0.05$).

Figure 1. Effect of β3-AR activation on body fat content, adipose tissue triglyceride content, and tissue weight. Mice (male, 8 weeks of age, n=4-8) were treated with the β3-AR agonist (CL) at 0.75nmol/hr for 7 days. Absolute (A) and relative (B) body fat was determined by MRI. (C)Triglyceride (TG) content of indicated adipose tissue depots after 1 (1D CL) and 7 days (7D CL) of CL treatment. (D) Absolute and (E) relative tissue weights after 7 days of CL treatment. Data were analyzed by two-way ANOVA (C) or t-test (A, B,C) to determine the effect of CL (***P < 0.001; **P < 0.01; *P < 0.05).

Downloaded from www.jlr.org by guest, on October 17, 2018

Figure 2. Effect of chronic β3-AR activation on lipid turnover and de novo lipogenesis in adipose tissues. Mice (male, 8 weeks of age, n=4-5) were treated with the β3-AR agonist for 1 (1D CL) or 7 (7D CL) days, and de novo synthesis of (A) palmitate and (B) glycerol in triglyceride was determined using the D₂O technique. Data were analyzed by two-way ANOVA to determine the effect of CL (***P < 0.001; *P < 0.05).

Figure 3. Chronic β 3-AR activation increases the expression of proteins involved in oxidation and lipogenesis in adipose tissue depots. Mice (male, 8 weeks of age, n=4) were treated with the β 3-AR agonist for 7 days (7D CL) and the expression of MCAD, UCP1, and FASN in BAT (A), iWAT (B) and gWAT (C) was assessed by western blot.

Figure 4. Inducible deletion of adipocyte ATGL prevents fat loss during chronic CL treatment. (A) Tamoxifen treatment induced deletion of ATGL in CreER^{T2}+ mice (iAAKO) but not in control mice. (B) FFA release was measured in isolated adipocytes from control or iAAKO mice under basal or stimulated conditions (Iso, CL) or (C) in serum of mice (male and female, 8-10 weeks of age, n=4) challenged with CL for 15 min. (D) WT (n=4-5) or iAAKO (n=4) mice were treated with the β3-AR agonist CL for 7 days (7D CL) and absolute and relative change in body fat was determined by MRI (&& notes an effect of iAAKO genotype on body fat). Absolute (E) and relative (F) adipose tissue weights of control and CL-treated control and iAAKO mice (&&& indicates a main effect of iAAKO genotype on fat pad weight by ANOVA; P < 0.001).

Downloaded from www.jlr.org by guest, on October 17, 2018

Figure 5. ATGL is required for elevation of de novo lipogenesis by β3-AR activation in adipose tissue depots. Control (male and female, 8-10 weeks of age, n=4) or iAAKO mice (male and female, 8-10 weeks of age, n=3) were treated with the β3-AR agonist CL for 7 days and de novo synthesis of (A) palmitate and (B) glycerol in triglyceride was determined using the D₂O technique. Data were analyzed by two-way ANOVA to determine the effect of CL (***P < 0.001; *P < 0.05; ns, non-significant).

Figure 6. Adipocyte ATGL differentially regulates the induction of FASN, PEPCK and GYK protein by β3-AR activation. Control (Ctl), or iAAKO mice (male and female, 8-10 weeks of age, n=4-5) were treated with CL for 7 days (7D CL) and the expression of FASN (A), PEPCK (B) and GYK (C) was determined by western blot. Data were analyzed by two-way ANOVA to

determine the effect of CL (***P < 0.001; **P < 0.01) or an overall effect of iAAKO ($^{\&\&}$ P < 0.01, $^{\&\&\&}$ P < 0.001).

Figure 7. Expansion of mitochondrial respiration by β3-AR agonist treatment requires adipocyte ATGL. (A) Mitochondrial respiration in adipose tissue depots (n=4-5) as determined by reduction of the electron acceptor dye TTC. Data were analyzed by two-way ANOVA to determine the effect of CL (***P < 0.001; **P < 0.01; *P < 0.05; ns, non-significant). (B) Adipose tissues from control or IAAKO mice treated with vehicle (Ctl) or CL for 7 days were collected and the mRNA expression of MCAD and UCP1 were measured by qPCR. (C) Western blot analysis and quantification of MCAD (D) and UCP1 (E) protein expression. Data were analyzed by two-way ANOVA to determine the effect of CL (***P < 0.001; **P < 0.01; *P < 0.05; ns, non-significant), or ATGL (*&*P < 0.01, *&&*P < 0.001).

Figure 8. Proposed model for coupling of lipid hydrolysis to oxidation and synthesis during chronic β3-AR stimulation. Stimulation of the β3-adrenergic receptor (β3-AR) by CL 316,243 (CL) leads to greater cAMP and activation of PKA which directly activates lipolysis by phosphorylating hormone sensitive lipase (HSL) and perilipin 1 (Plin1), and indirectly by releasing the co-activator α-β hydrolase domain containing 5 (Abhd5) which binds to adipose triglyceride lipase (ATGL). At the gene regulatory level, transcriptional activity can be potentially (dashed lines) activated by PKA directly phosphorylating cAMP response element binding protein (CREB), or by ATGL-dependent generation of ligands for peroxisome proliferator-activated receptors (PPARs) to upregulate the expression of genes involved in lipid synthesis (fatty acid synthase, FASN; phosphoenolpyruvate carboxykinase, PEPCK; glycerol kinase, GYK). Greater flux of substrate (glucose; TCA cycle intermediates from mitochondria, not shown) and increased protein levels of enzyme involved in de novo lipogenesis (FASN), glyceroneogenesis (PEPCK) and glycerol recycling (GYK), translates into greater lipid turnover which is coupled to lipid oxidation and uncoupling. TG, triglyceride.

Downloaded from www.jlr.org by guest, on October 17, 2018

Table 1: Chronic stimulation of β 3-ARs increases the expression of genes involved in oxidation (LCAD, Cox8b and UCP1), lipogenesis (FASN, SCD1, ACLY and ACC1) and glycerol turn over (Gyk and PEPCK) in adipose tissue depots.

בֿ	ıe	gWAT (% PPIA)			iWAT (% PPIA)			BAT (% PPIA)		
		CON	1D CL	7D CL	CON	1D CL	7D CL	CON	1D CL	7D CL
à	Ď	1.7±0.2	2.7±1.1	8.5±0.5***	2.7±0.3	5.7±0.8	6.7±1.0 ^{&}	70.2±3.2	53.1±4.8	66.2±6.1
	8b	2.0±0.8	2.0±1.6	37.3±6.5***	10.3±0.7	29.4±10.8	51.2±5.2 ^{&&}	439±20.8	191±10 ^{##}	312±24***
	1	0.6±0.5	0.9±0.2	2.6±1.5	0.1±0.04	25.8±8.1 [#]	17.6±4.7	212±24.2	590±117 [#]	446±48.3
	N	1.4±0.9	0.5±0.3	11.4±4.0*	4.6±1.8	0.6±0.2	6.6±1.6 ^{\$}	15.8±7.7	4.7±1.5	52.6±8.5*
)1	196.5±37	81.8±17.1	791±98***	194±26	53.9±14 [#]	200±47.8 ^{\$}	439±65	206±42.8	816±76g*
	.Y	5.2±2.0	2.5±0.3	19.4±3.5**	8.4±2.9	1.4±0.4	10.3±1.9 ^{\$}	19.1±9.2	6.0±1.8	34±8.5
	; 1	1.5±0.2	0.5±0.2 [#]	2.3±0.2 ^{&&&}	1.8±0.2	0.3±0.1 ^{###}	1.2±0.1 ^{\$\$}	7.0±2.7	2.5±0.6	11.4±2;6
	k	1.1±0.34	14.9±3.1 ^{##}	2.8±0.5 ^{&&}	0.6±0.1	26.3±7 ^{###}	6.5±1.7 ^{&&}	5.7±0.4	11.9±1 ^{###}	5.7±0.7 §
	CK	69.3±15	31.4±12.7	228.5±67*	192±44	88.9±9.1	149±37.6	115.9±14	47.6±1.8 ^{##}	84.1±7 gg
										ctober 17, 2018

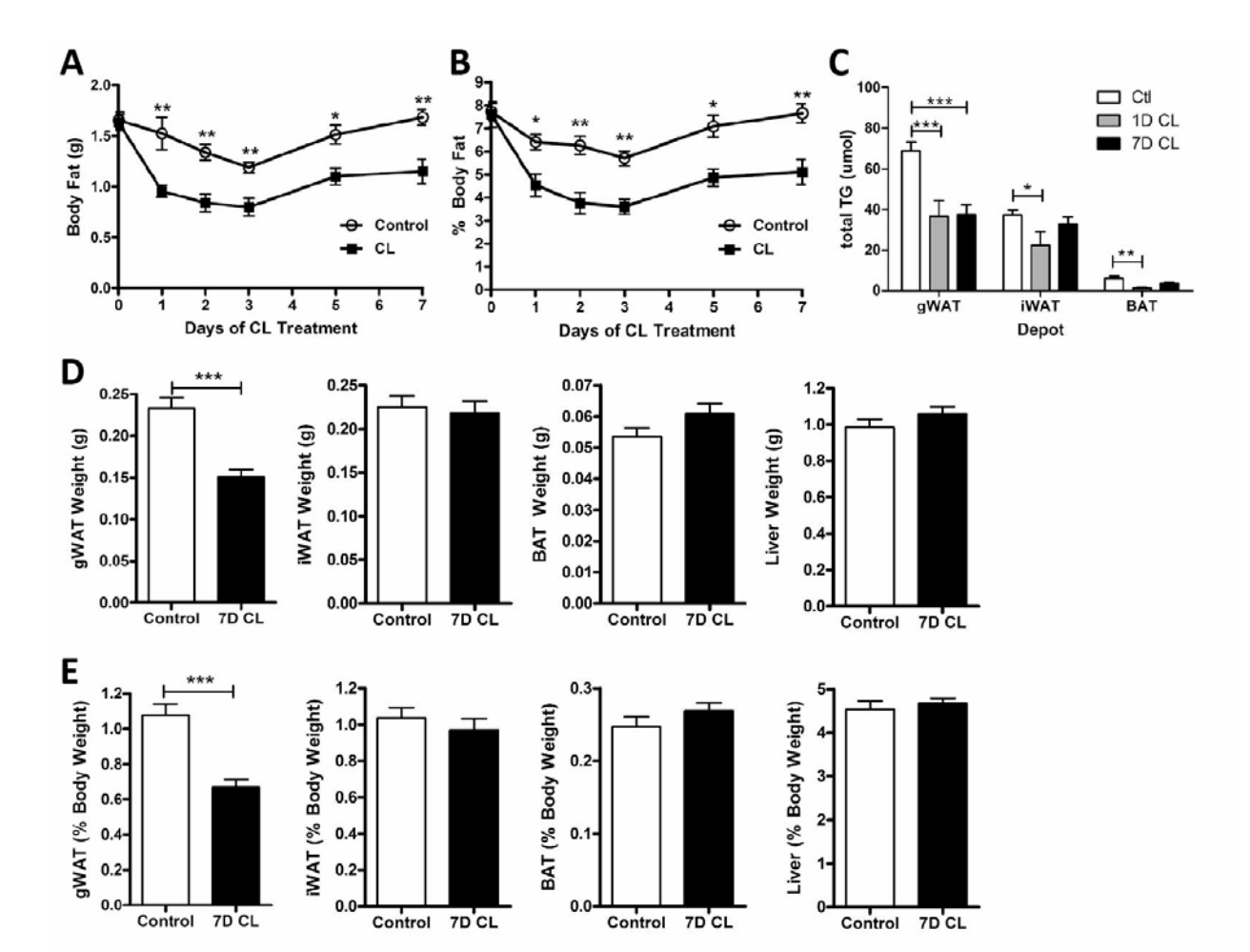
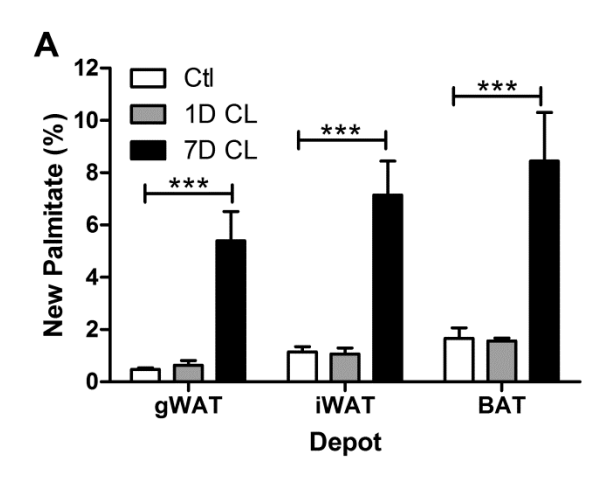


Figure 1



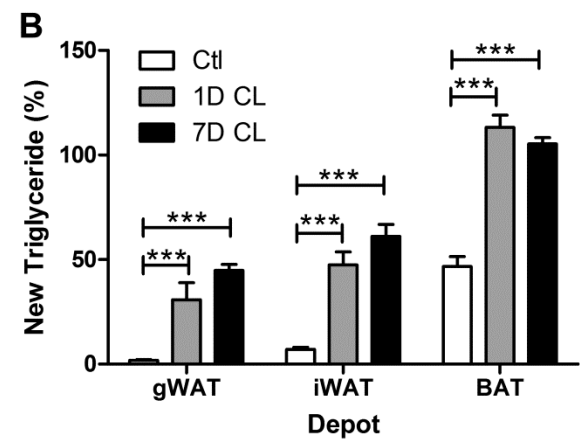


Figure 2

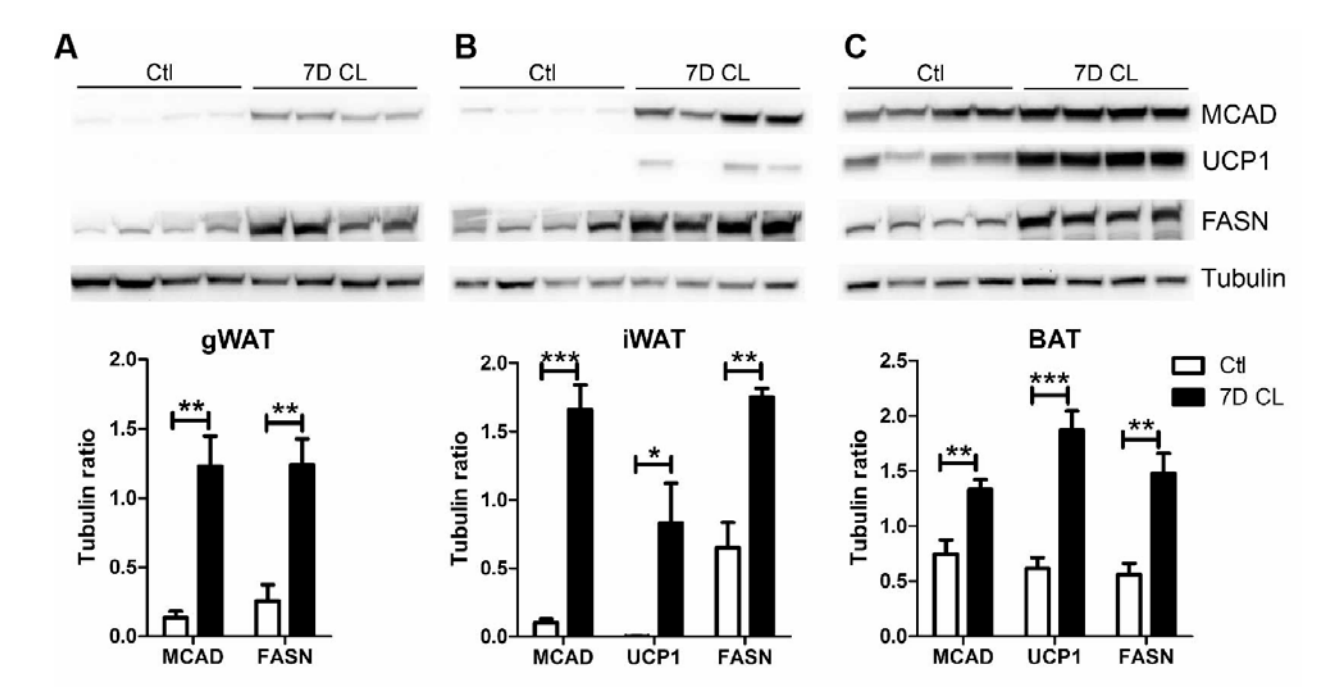


Figure 3

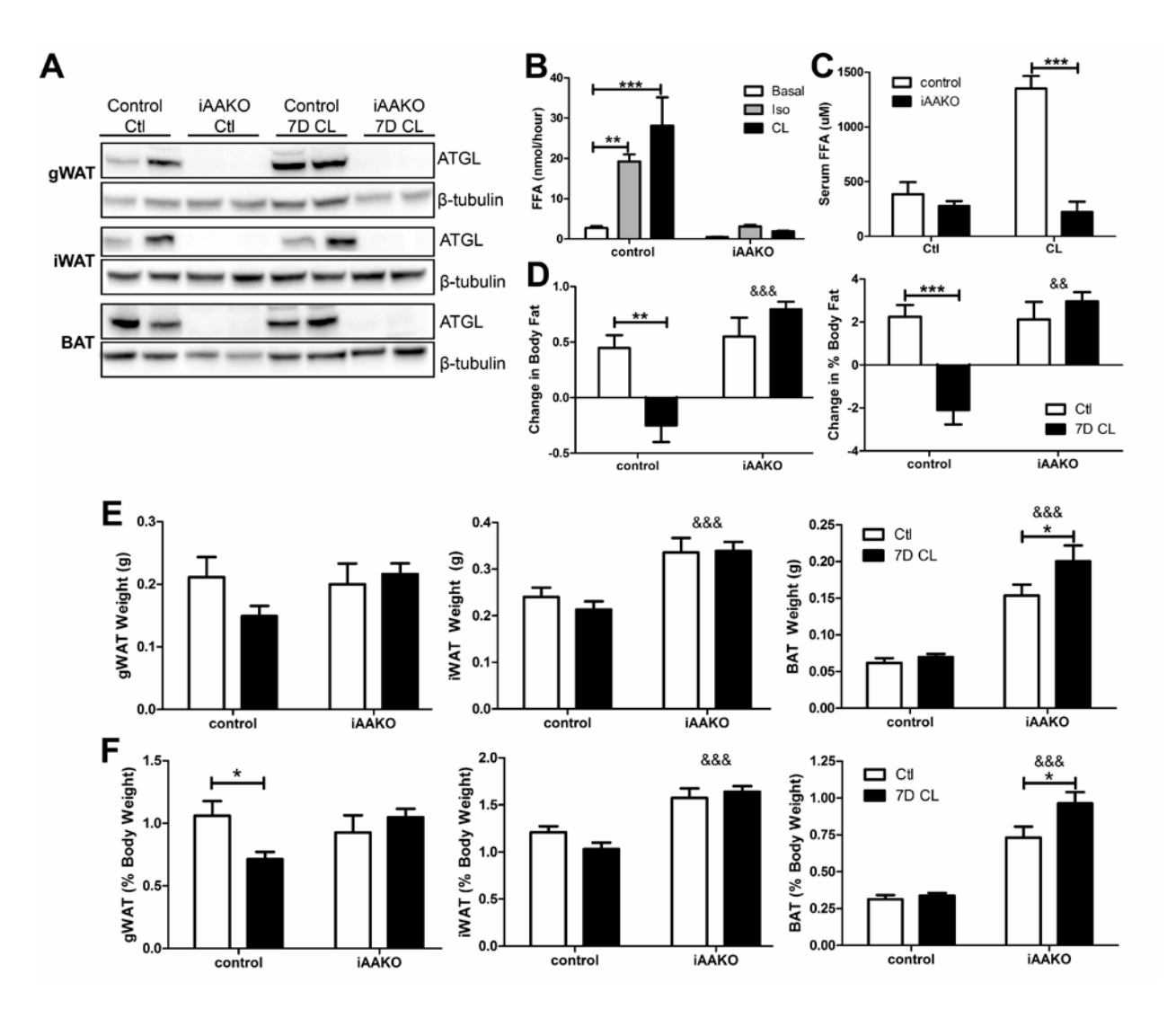


Figure 4



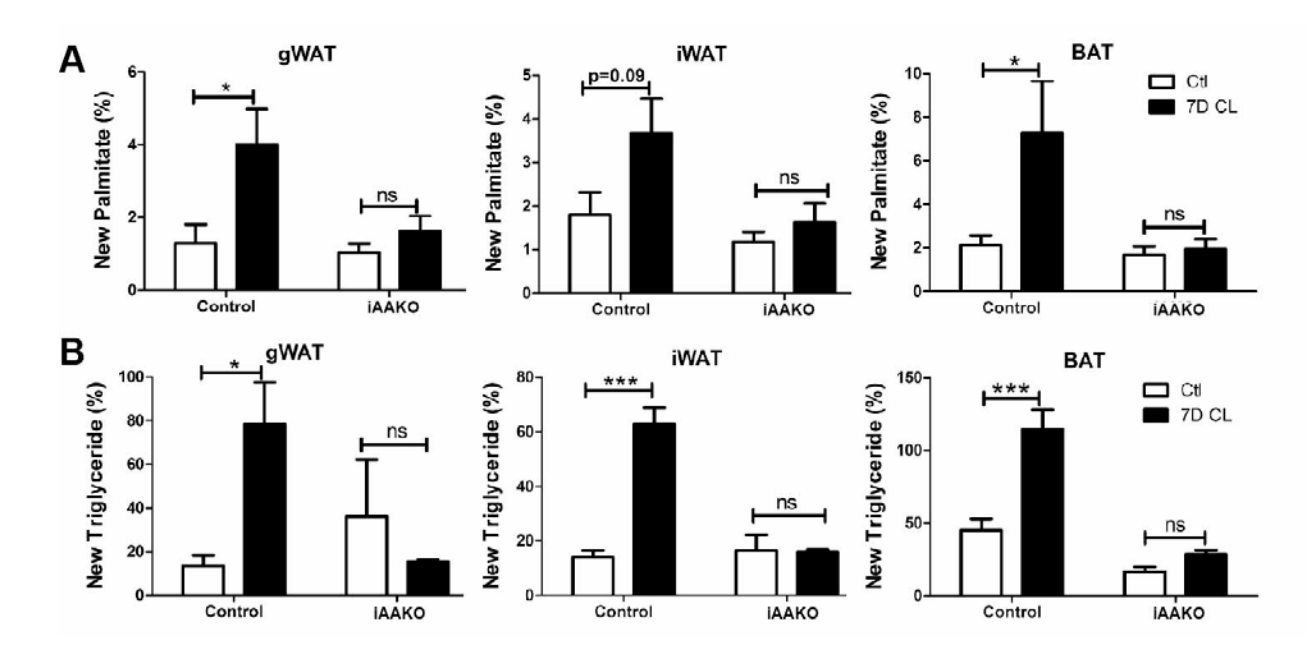


Figure 5

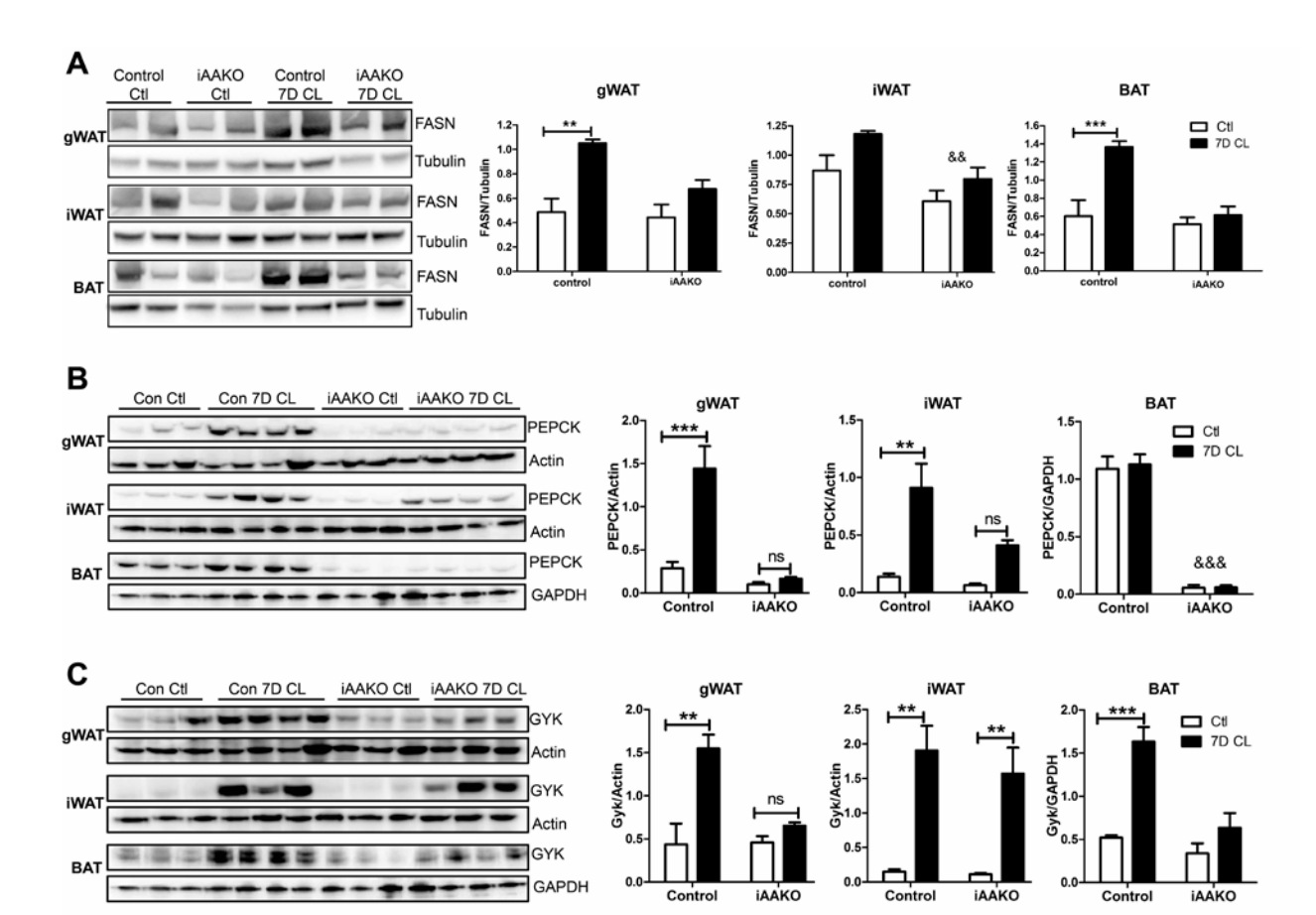


Figure 6

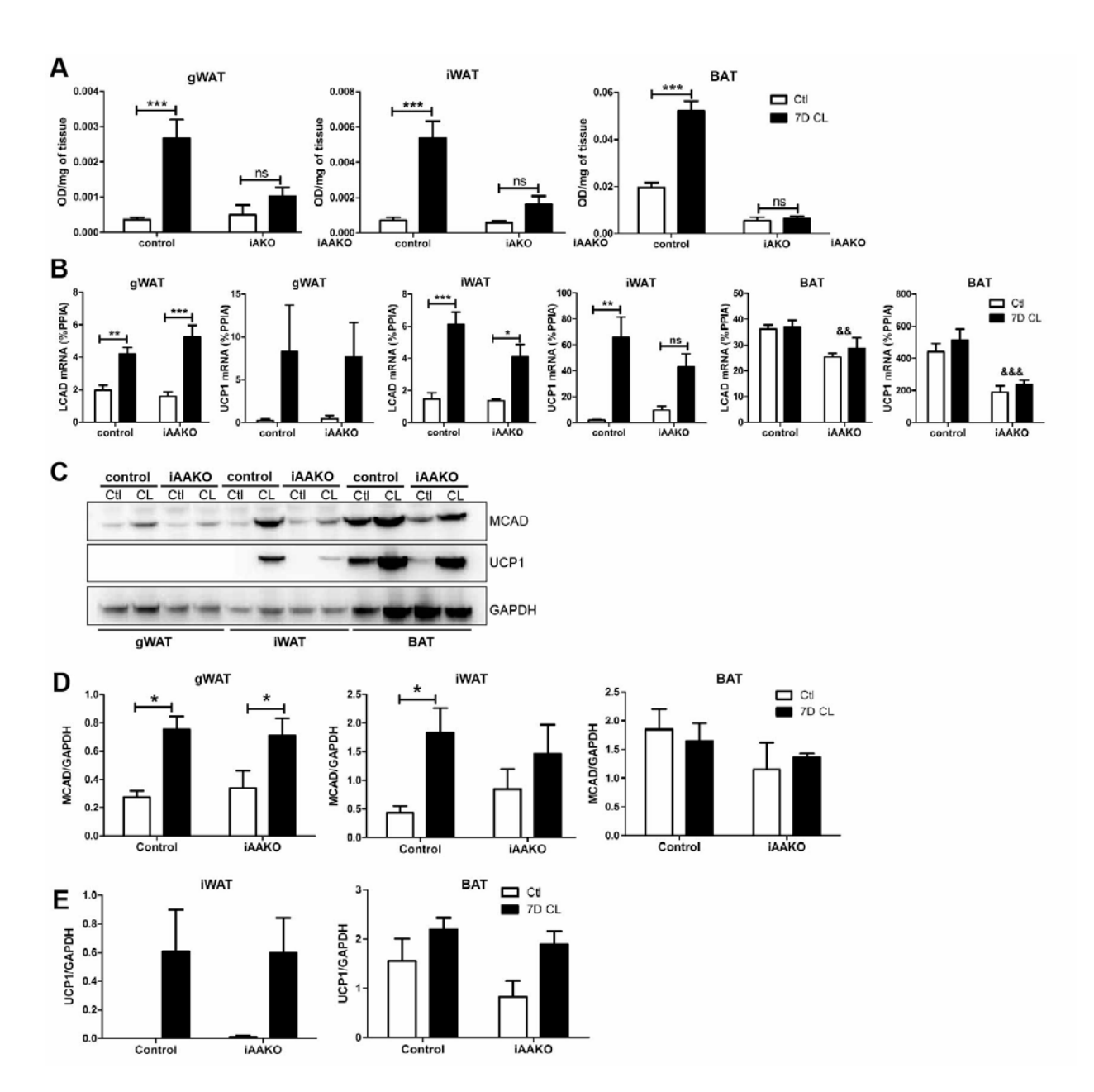


Figure 7

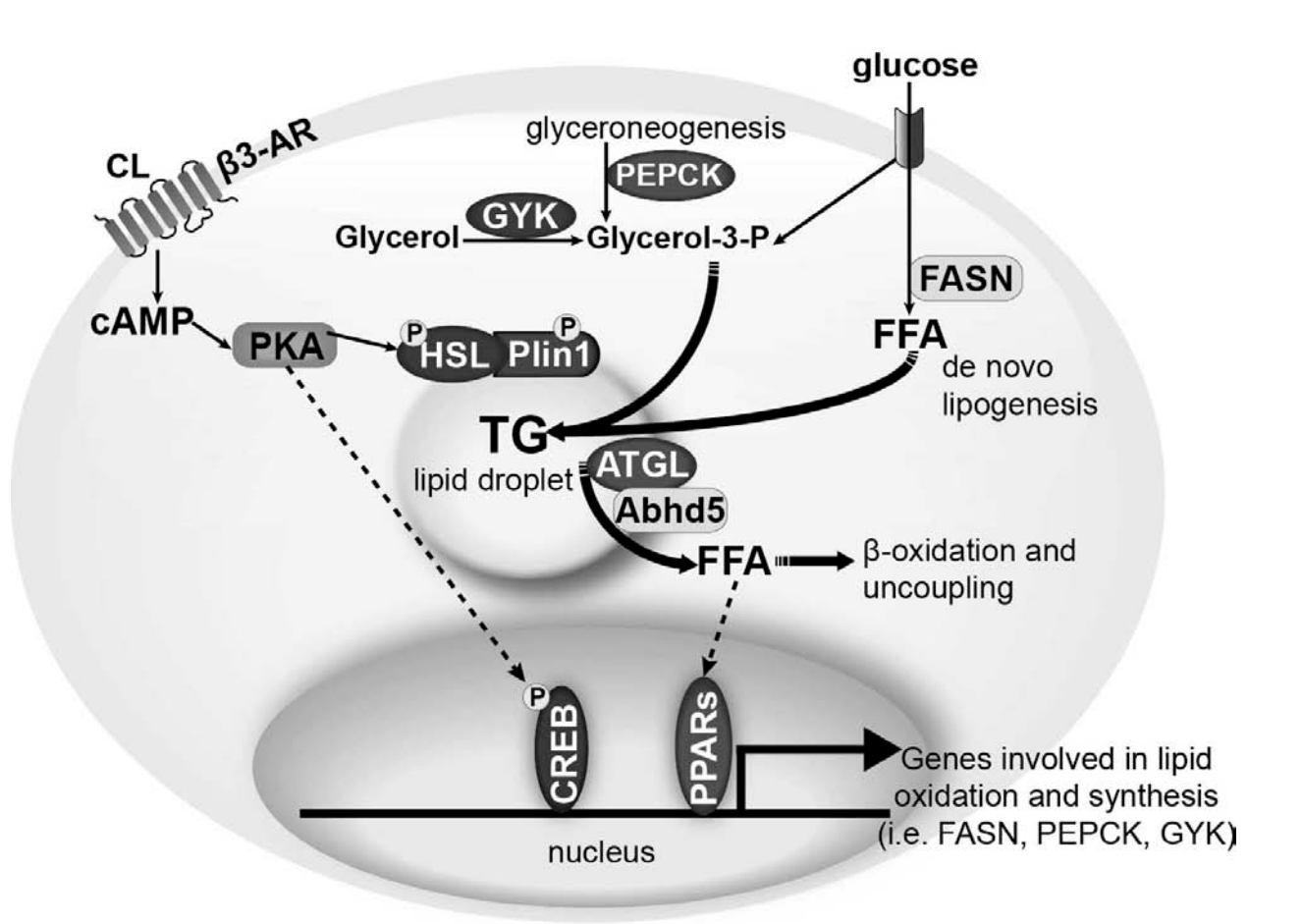


Figure 8